Electron-Pair Resonance in the Coulomb Blockade

Eran Sela,[1] H.-S. Sim,[2] Yuval Oreg,[1] M. E. Raikh,[3] and Felix von Oppen[4]

[1]*Department of Condensed Matter Physics, Weizmann Institute of Science, Rehovot, 76100, Israel*
[2]*Department of Physics, Korea Advanced Institute of Science and Technology, Daejeon 305-701, Korea*
[3]*Department of Physics, University of Utah, Salt Lake City, Utah 84112, USA*
[4]*Institut für Theoretische Physik, Freie Universität Berlin, Arnimallee 14, 14195 Berlin, Germany*

We study many-body corrections to the cotunneling current via a localized state with energy ϵ_d at large bias voltages V. We show that the transfer of *electron pairs*, enabled by the Coulomb repulsion in the localized level, results in ionization resonance peaks in the third derivative of the current with respect to V, centered at $eV = \pm 2\epsilon_d/3$. Our results predict the existence of previously unnoticed structure within Coulomb-blockade diamonds.

Introduction.—Current flow through a single localized state (LS) coupled to metallic leads is a paradigm of quantum transport through nanostructures, with applications to many systems such as impurities embedded in tunnel barriers, quantum dots, single-molecule junctions, or carbon nanotubes; see, e.g., Refs. [1–4]. Despite its simplicity, this system exhibits a wide range of transport behaviors, including resonant and sequential tunneling, cotunneling, and the Kondo effect.

All of these regimes are captured remarkably well by a simple extension of the Anderson impurity model

$$H = \sum_\sigma \epsilon_d d_\sigma^\dagger d_\sigma + U n_\uparrow n_\downarrow + \sum_{\mathbf{k}\sigma\alpha} \epsilon_\mathbf{k} c_{\mathbf{k}\sigma\alpha}^\dagger c_{\mathbf{k}\sigma\alpha}$$
$$+ \sum_{\mathbf{k}\sigma\alpha} [t_\alpha d_\sigma^\dagger c_{\mathbf{k}\sigma\alpha} + t_\alpha^* c_{\mathbf{k}\sigma\alpha}^\dagger d_\sigma], \quad (1)$$

which describes tunneling of amplitude t_α between the spin-degenerate LS of energy ϵ_d (with creation operator $d_{\sigma=\uparrow,\downarrow}^\dagger$ and number operator $n_\sigma = d_\sigma^\dagger d_\sigma$) and two leads $\alpha = L, R$ (with dispersion $\epsilon_\mathbf{k}$ and creation operator $c_{\mathbf{k}\sigma\alpha}^\dagger$). For large on-site Coulomb repulsion U, double occupation of the LS is suppressed and the nature of transport depends on both ϵ_d (tunable by a gate voltage V_g) and the bias voltage V. Within the shaded areas of the stability diagram in Fig. 1, the average occupation $n_d = n_\uparrow + n_\downarrow$ of the LS is close to integer and current flow is suppressed by the Coulomb blockade. In contrast, current can flow by sequential-tunneling processes outside the shaded areas, where the average occupation of the dot is no longer integer. This picture of the Coulomb blockade has been confirmed experimentally for various systems [1–4].

It is the main point of this Letter that even the minimal model of Eq. (1) predicts additional structure *within* the Coulomb-blockaded region, emerging from *two-electron* ionization of the LS at large biases. This ionization process is an effect of many-body correlations, enabled by the on-site Coulomb repulsion, which is much more robust than the Kondo correlations emerging in the Kondo valley $n_d = 1$ at low temperatures and small voltages. Indeed, the fine

structure due to the two-electron ionization process exists in both Kondo and non-Kondo valleys, as illustrated in Fig. 1.

The two-electron ionization requires biases beyond a threshold voltage V_c (see the thick lines in Fig. 1). Below the threshold voltage, correlated *two-electron* transfers between the two leads constitute a precursor effect to two-electron ionization. While the limit of the Coulomb-blockaded region is characterized by a resonance peak in the differential conductance dI/dV, we find that the onset of two-electron ionization at V_c is accompanied by a peak in d^3I/dV^3 [5]. Interestingly, the difference between both resonance phenomena emerges solely from familiar Fermi-liquid phase space factors which appear in the two-electron ionization rate. One important implication of this analogy is that the onset of two-electron ionization is accompanied by anomalous temperature sensitivity, even when $eV_c \gg T$, as is familiar for the boundary of the Coulomb-blockaded region.

Most of our predictions for the single LS extend to a metallic dot with essentially zero level spacing where the stability diagram exhibits a sequence of Coulomb diamonds, reflecting the stepwise population of the dot with
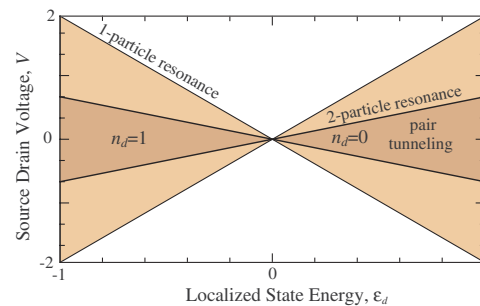

FIG. 1 (color online). Schematic stability diagram of a single-level quantum dot. The thick lines within the shaded Coulomb-blockaded region are characterized by a resonance peak in d^3I/dV^3 due to opening of two-electron ionization. For eV below the threshold voltage $eV_c = 2\epsilon_d/3$, tunneling of electron pairs is a precursor effect to two-electron ionization.

increasing gate voltage. It is easy to see that for the metallic dot, the boundaries of two-electron ionization translate into a sequence of *inner diamonds*. This is depicted in Fig. 2, where we include the effects of asymmetric capacitances between dot and electrodes.

In the remainder of the Letter, we quantify the behavior of the current near the two-particle threshold.

Two-electron ionization.—Ionization by means of single-particle tunneling becomes energetically allowed when the source chemical potential $eV/2$ is aligned with the LS, i.e., at $eV = \pm 2\epsilon_d$. In contrast, the two-particle ionization process, responsible for the predicted boundaries in the stability diagram, is depicted in Fig. 3(a). At finite bias, an electron tunneling between the leads can suffer an energy loss up to eV. Because of the on-site Coulomb repulsion, this energy loss can be transferred to a second electron from the source electrode, exciting it to energies up to $3eV/2$. Specifically, the second electron can populate (and thus ionize) the LS once its maximal energy exceeds ϵ_d, i.e., for biases exceeding the threshold voltage

$$eV_c = 2\epsilon_d/3. \qquad (2)$$

The predicted lines in the stability diagram originating from the onset of two-electron ionization occur for $V = \pm V_c$. Thus, they are located *within* the Coulomb-blockaded region which extends up to $eV = \pm 2\epsilon_d$.

Microscopically, the two-electron ionization process proceeds as follows, cf. Fig. 3(a): (i) An electron with energy ϵ_1 from the source electrode (L) enters the LS and (ii) tunnels into the state E_1 of the drain (R). In the *same* process, (iii) a second electron with opposite spin and energy ϵ_2 tunnels from the source into the LS. The amplitudes of steps (i) and (iii) are proportional to t_L, while that of step (ii) is proportional to t_R^*. Thus, the ionization
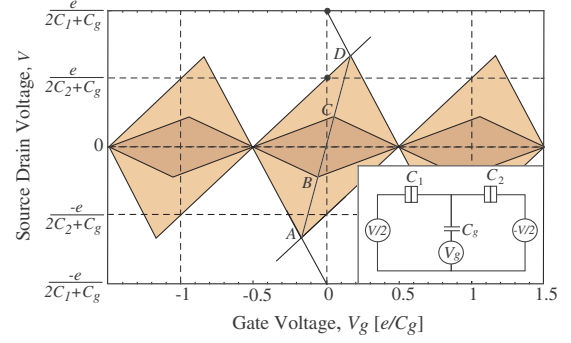

FIG. 2 (color online).   Stability diagram of a metallic quantum dot with vanishing level spacing. The threshold lines for two-electron ionization can be determined by examining the electrostatic energy of the circuit. Graphically they are obtained (e.g., for the central diamond) by rescaling the diagonal $\overline{AD}$ by a factor 3, so that $\overline{AB} = \overline{BC} = \overline{CD}$. Inset: Equivalent electric circuit for a metallic island.

amplitude is given by

$$A^{\epsilon_2 \to \epsilon_d}_{\epsilon_1 \to E_1} = \frac{t_L^2 t_R^*}{(\epsilon_d - \epsilon_1)(E_1 - \epsilon_1)}. \qquad (3)$$

Following standard perturbation theory, the energy denominators are given by the difference between the intermediate and initial energies. In Eq. (3), we assumed a large on-site Coulomb repulsion U so that there is no contribution from virtual states with double occupation of the LS. If these states were included, the corresponding terms would exactly cancel the amplitude in Eq. (3) in the limit of vanishing U. This shows that two-electron ionization is enabled by the on-site interaction.

Based on Eq. (3) and energy conservation, the two-electron ionization rate per spin, at $T = 0$, is

$$\Gamma_{\rm ion} = \frac{\Gamma_L^2 \Gamma_R}{(2\pi)^2} \int_{-\infty}^{eV/2} d\epsilon_1 \int_{-\infty}^{eV/2} d\epsilon_2 \int_{-eV/2}^{\infty} dE_1 \frac{1}{(\epsilon_d - \epsilon_1)^2 (\epsilon_2 - \epsilon_d)^2} \delta(\epsilon_1 + \epsilon_2 - \epsilon_d - E_1), \qquad (4)$$

where $\hbar = 1$. Here $\Gamma_L = 2\pi |t_L|^2 \nu$ and $\Gamma_R = 2\pi |t_R|^2 \nu$ are the partial widths of the LS due to escape to source and drain, respectively, and ν denotes the density of states in the leads. Performing the integration over ϵ_2, we obtain

$$\Gamma_{\rm ion} = \frac{\Gamma_L^2 \Gamma_R}{(2\pi)^2} \int_{-\infty}^{eV/2} d\epsilon_1$$
$$\times \int_{-eV/2}^{\infty} dE_1 \frac{\theta(eV/2 + \epsilon_1 - E_1 - \epsilon_d)}{(\epsilon_d - \epsilon_1)^2 (E_1 - \epsilon_1)^2}, \qquad (5)$$

where $\theta(x)$ is the step function. Since $-eV/2 < E_1$ and $\epsilon_1 < eV/2$, the argument of the $\theta(x)$ function is negative for $\epsilon_d > 3eV/2$, i.e., for $eV < eV_c$. In contrast, for $0 < V - V_c \ll V_c$, the integration regions for ϵ_1 and E_1 are restricted to $\epsilon_d - eV < \epsilon_1 < eV/2$ and $-eV/2 < E_1 < eV - \epsilon_d$, respectively. Since both regions are narrow, we find the threshold behavior

$$\Gamma_{\rm ion} = \frac{9\Gamma_L^2 \Gamma_R (V - V_c)^2}{32\pi^2 e^2 V_c^4} \theta(V - V_c) \qquad (6)$$

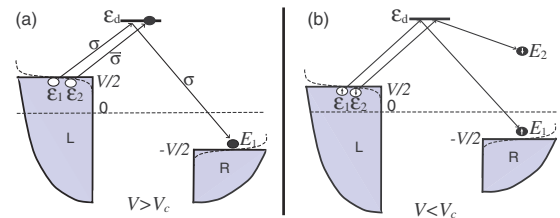of the two-electron ionization rate $\Gamma_{\rm ion}$.

FIG. 3 (color online).   Schematic rendering of (a) two-electron ionization of the LS, in which one electron tunnels from source to drain while the other jumps into the LS, and (b) pair tunneling, in which two electrons tunnel between source and drain. Both processes are enabled by the on-site Coulomb repulsion suppressing double occupation of the LS.

It is crucial that energy exchange between electrons in the leads does *not* require direct interaction between them. Instead, this process is enabled by the finite Coulomb repulsion in the LS alone. In this regard, the underlying physics of two-particle ionization is similar to that of energy exchange between electrons in a bulk metal, facilitated by a magnetic impurity [6]. Indeed, it is the nonzero on-site Coulomb repulsion U that ultimately generates the magnetic impurity [7]. Curiously, similar processes can also be enabled by the pairing interaction in devices of two Josephson junctions in series, where they lead to subgap structure in the current [8].

After entering the empty LS with rate Γ_{ion} by two-electron ionization, the electron rapidly escapes into source or drain electrode by single-electron tunneling, with rates Γ_L and Γ_R, respectively. Then, the average occupation of the LS is governed by the rate equation $2\Gamma_{\text{ion}}(1 - n_\uparrow) \times (1 - n_\downarrow) = (\Gamma_L + \Gamma_R)n_d$, which yields $n_d \simeq 2\Gamma_{\text{ion}}/(\Gamma_L + \Gamma_R)$). Since the net charge transfer is $2e$ (e) when the electron tunnels out to the drain (source) electrode, the "two-electron ionization" current $I(V)$ between the leads becomes

$$I(V) = e(2\Gamma_R + \Gamma_L)n_d \approx 2e\Gamma_{\text{ion}}\frac{2\Gamma_R + \Gamma_L}{\Gamma_L + \Gamma_R}. \quad (7)$$

Because of Γ_{ion}, the ionization current $I(V)$ also exhibits the threshold behavior $I(V) \propto (V - V_c)^2\theta(V - V_c)$.

Clearly, the ionization current, Eqs. (6) and (7), constitutes but a small fraction $\sim\Gamma_L(V - V_c)^2/V_c^3$ of the cotunneling current $\sim \frac{\Gamma_L\Gamma_R}{\epsilon_d^2}V$. Thus, it is an important question how the threshold anomaly Eq. (7) can be distinguished from the background cotunneling current. Equation (7) predicts that two-electron ionization induces a jump in d^2I/dV^2 located at $V = V_c$. We now turn to a more careful analysis of this jump, focusing first on the two-electron current below threshold, before deriving a general interpolation formula.

Two-electron current below threshold.—For voltages below the threshold, $V < V_c$, ionization of the LS is no longer possible by two-electron processes. But two-electron processes can still excite electrons in the leads to just below the energy of the LS. We will now show that this constitutes a precursor effect to two-electron ionization which contributes a logarithmically singular threshold dependence to the differential conductance.

For large on-site Coulomb repulsion U, the two-electron process below threshold proceeds microscopically as follows, cf. Fig. 3(b): (i) A spin-up electron from lead α_1 with energy ϵ_1 enters the LS; (ii) the electron tunnels out to state E_1 in lead α_1'; (iii) a spin-down electron from lead α_2 with energy ϵ_2 enters the LS, and (iv) leaves into state E_2 in lead α_2'. The corresponding amplitude is

$$A_{\epsilon_2 \to E_2}^{\epsilon_1 \to E_1} = \frac{t_{\alpha_1}t_{\alpha_2}t_{\alpha_1'}^*t_{\alpha_2'}^*}{(\epsilon_d - \epsilon_1)(E_1 - \epsilon_1)(\epsilon_d - E_2)} + (1 \leftrightarrow 2), \quad (8)$$

where the second term accounts for the four-step process described above with the interchanged order (iii) $\mapsto$ (iv) $\mapsto$ (i) $\mapsto$ (ii). This results in a scattering rate

$$\Gamma_{\alpha_2 \to \alpha_2'}^{\alpha_1 \to \alpha_1'} = 2\pi\nu^4 \int \prod_{i=1}^{2}[d\epsilon_i dE_i f(\epsilon_i - \mu_{\alpha_i})$$
$$\times \{1 - f(E_i - \mu_{\alpha_i'})\}] \left| A_{\epsilon_2 \to E_2}^{\epsilon_1 \to E_1} \right|^2$$
$$\times \delta(\epsilon_1 + \epsilon_2 - E_1 - E_2). \quad (9)$$

Here $f(\epsilon) = [e^{\epsilon/T} + 1]^{-1}$ and $\mu_{L/R} = \pm eV/2$. The resulting two-electron tunneling current is $I = I^{(1e)} + I^{(2e)}$, where $I^{(2e)} = 2e\Gamma_{L \to R}^{L \to R}$ corresponds to two-electron transfer between the leads, while $I^{(1e)} = e\sum_\alpha(\Gamma_{\alpha \to \alpha}^{L \to R} + \Gamma_{L \to R}^{\alpha \to \alpha})$ accounts for one-particle transfer between the leads, accompanied by the creation of a particle-hole excitation in one lead.

The crucial observation is that I is *singular* as V approaches V_c from below. The singularity arises from the domain $E_1 \simeq -eV/2$, $E_2 \simeq 3eV/2$, $\epsilon_1 \simeq \epsilon_2 \simeq eV/2$. To see this, we first note that in this domain, the amplitude $A_{\epsilon_2 \to E_2}^{\epsilon_1 \to E_1}$ simplifies, $A_{\epsilon_2 \to E_2}^{\epsilon_1 \to E_1} \simeq \frac{-t_{\alpha_1}t_{\alpha_2}t_{\alpha_1'}^*t_{\alpha_2'}^*}{(eV_c)^2(\epsilon_d - E_2)}$. Using the golden rule Eq. (9), and performing the integrals over ϵ_1, ϵ_2, and E_1, we obtain for $eV_c \gg T$

$$I = \frac{2e}{h}\frac{\Gamma_L^2\Gamma_R(\Gamma_R + \frac{1}{2}\Gamma_L)}{(2\pi)^2(eV_c)^4}\int dE_2 \frac{1 - f(E_2 + eV/2)}{(\epsilon_d - E_2)^2}$$
$$\times f(E_2 - 3eV/2)[(\pi T)^2 + (E_2 - 3eV/2)^2]. \quad (10)$$

Since both E_2 and ϵ_d in the denominator of Eq. (10) are close to $3eV/2$, the remaining integration yields the singular contribution

$$\frac{dI}{dV} = \frac{2e^2}{h}\frac{3\Gamma_L^2\Gamma_R(\Gamma_R + \frac{1}{2}\Gamma_L)}{(2\pi)^2(eV_c)^4}\ln\frac{eV_c}{\max\{eV_c - eV, T\}} \quad (11)$$

to the differential conductance. The logarithmic singularity in the two-electron tunneling current at V_c signals the opening of the two-particle ionization channel in Eq. (7) which is lower order in the tunneling amplitudes and involves *real* occupation of the LS.

The appearance of T dependence in Eq. (11) at $eV_c \gg T$ resembles the behavior of the conductance near the onset of sequential tunneling at $eV = \pm 2\epsilon_d$, cf. Fig. 1. In fact, we find that the analogy between the onset of sequential tunneling at $eV = \pm 2\epsilon_d$ and the onset of two-electron ionization at $V = \pm V_c$ goes much further. The lines $eV = \pm 2\epsilon_d$ in the stability diagram separate transport regimes with real occupation (sequential tunneling) and virtual occupation (cotunneling) of the LS. Similarly, the lines $V = \pm V_c$ separate regimes with real occupation (two-electron ionization) and virtual occupation (pair tunneling) of the LS. We now explore this analogy on a quantitative level.

Correspondence of one-electron and two-electron ionization.—We start by noting that Eqs. (7) and (11) yield

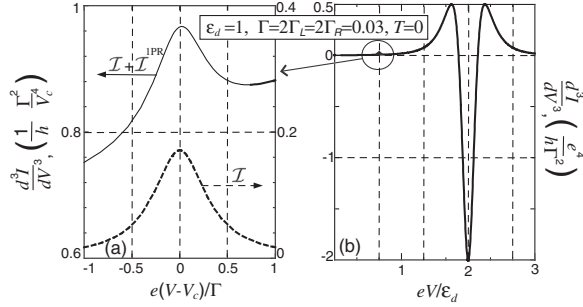FIG. 4.   (a) The two-particle resonance induces a peak (dashed line) in $d^3 I/dV^3$ of width $\max(T, \Gamma)$, centered at $V = V_c$. The full-line curve shows that the two-particle resonance can be observed on top of the smoothly varying single-particle background. (b) The single-particle contribution to $d^3 I^{1PR}/dV^3$ becomes singular at $eV = 2\epsilon_d$.

$d^2 I/dV^2 \propto \theta(V - V_c)$ and $d^2 I/dV^2 \propto 1/(V_c - V)$, which are the familiar voltage dependencies of the sequential-tunneling and cotunneling currents, respectively, provided we make the replacement $eV_c \leftrightarrow 2\epsilon_d$. This suggests that the currents near the onsets of sequential tunneling and two-electron ionization are related to one another more generally by two voltage derivatives. To establish this relation, although approximately, we incorporate the lifetime broadening $\Gamma = \Gamma_L + \Gamma_R$ of the LS into Eq. (10), and cast it into the form

$$I \simeq \frac{2e}{h} \frac{\Gamma_L^2 \Gamma_R(\Gamma_R + \frac{1}{2}\Gamma_L)}{(2\pi)^2 (eV_c)^4} \int \frac{d\epsilon\{f(\epsilon - eV) - f(\epsilon + eV)\}}{[\epsilon - (\epsilon_d - eV/2)]^2 + (\Gamma/2)^2}$$
$$\times [(\pi T)^2 + (\epsilon - eV)^2], \qquad (12)$$

where $\epsilon \equiv E_2 - eV/2$. The finite lifetime provides a physical cutoff of the singularity in Eq. (11). Most importantly, Eq. (12) captures processes involving *both* virtual and real occupations of the LS, i.e., it describes the *two-electron resonance*. Indeed, it can be easily verified that the above and below-threshold limits, Eqs. (7) and (10), of the pair resonance are reproduced by Eq. (12). For $V \sim V_c$, Eq. (12) constitutes an approximate interpolation formula, due to the attachment of an energy-independent width Γ to the two-particle resonance.

We compare Eq. (12) with a single-particle resonance

$$I^{1PR}[V, \epsilon_d] = \frac{2e}{h} \Gamma_L \Gamma_R \int d\epsilon \frac{f(\epsilon - \frac{eV}{2}) - f(\epsilon + \frac{eV}{2})}{(\epsilon - \epsilon_d)^2 + (\Gamma/2)^2}.$$

The qualitative difference between the two expressions arises from the appearance of the Fermi-liquid phase space factor $[(\pi T)^2 + (\epsilon - eV)^2]$ in the two-particle resonance Eq. (12). This phase space factor can be removed by taking two derivatives with respect to voltage of Eq. (12). In this way, we find the relation

$$\frac{d^3 I}{dV^3} \simeq \frac{\Gamma_L(2\Gamma_R + \Gamma_L)}{(2\pi)^2 e^2 V_c^4} \frac{d}{dV} I^{1PR}[2V, \epsilon_d - eV/2], \quad (13)$$

with the explicit replacements $V \rightarrow 2V$ and $\epsilon_d \rightarrow$

$\epsilon_d - eV/2$. In view of the known properties of the single-particle resonance, this result constitutes our principal prediction. For $T \ll \Gamma$, Eq. (13) predicts a Lorenzian peak in $d^3 I/dV^3$ inside the Coulomb-blockade diamond. Importantly, at $V = V_c$ both $d^3 I/dV^3$ and $d^3 I^{1PR}/dV^3$ have the same order of magnitude $\sim \Gamma^2/(hV_c^4)$. These results are illustrated in Fig. 4. Note that, for $T \gg \Gamma$, Eq. (13) also predicts temperature broadening of the peak in $d^3 I/dV^3$.

Discussion and conclusion.—Previously it was believed that in the course of cotunneling through a LS, electrons from the source arrive at the drain *one by one*. Here we demonstrated that there exists a well-pronounced, although more delicate, transport regime where two-electron processes (of opposite spin) contribute to the current. We emphasize that this regime is captured by the standard Anderson Hamiltonian (1).

Intriguingly, our reasoning is easily extended to regimes associated with N-particle ionization of the LS ($N > 2$). These induce additional boundaries in the stability diagram Fig. 1 at even lower voltages $eV < eV_c^{(N)} = 2\epsilon_d/(2N - 1)$. A naive estimate of the corresponding near-threshold behavior of the current gives $\sim \theta(V - V_c^{(N)})[\Gamma^{2N-1}(eV - eV_c^{(N)})^{2(N-1)}/(eV_c^{(N)})^{4(N-1)}]$. However, destructive interference between different sequences of N-electron transitions might lead to further reduction of the current.

Throughout this Letter, we considered an empty LS at zero bias (non-Kondo valley $\epsilon_d > 0$). The analysis of the ionization process of the occupied LS (Kondo valley $\epsilon_d < 0$) is entirely analogous, and differs only by the order of virtual transitions.

[1] M. A. Kastner, Rev. Mod. Phys. **64**, 849 (1992).
[2] L. Kouwenhoven and C. Marcus, Phys. World **11**, 35 (1998); L. Kouwenhoven and L. I. Glazman, *ibid.* **14**, 33 (2001).
[3] J. Park *et al.*, Nature (London) **417**, 722 (2002); W. Liang *et al.*, *ibid.* **417**, 725 (2002); A. N. Pasupathy *et al.*, Science **306**, 86 (2004).
[4] M. Bockrath *et al.*, Science **275**, 1922 (1997).
[5] $d^3 I/dV^3$ was measured, e.g., in T. Bergsten, T. Claeson, and P. Delsing, Appl. Phys. Lett. **78**, 1264 (2001).
[6] A. Kaminski and L. I. Glazman, Phys. Rev. Lett. **86**, 2400 (2001).
[7] P. W. Anderson, Phys. Rev. **124**, 41 (1961).
[8] A. Maassen van den Brink, G. Schön, and L. J. Geerligs, Phys. Rev. Lett. **67**, 3030 (1991); P. Hadley *et al.*, Phys. Rev. B **58**, 15 317 (1998).